Pergamon

DROPLET FLUX DISTRIBUTIONS AND ENTRAINMENT IN HORIZONTAL GAS–LIQUID FLOWS

L. R. WILLIAMS, L. A. DYKHNO and T. J. HANRATTY

University of Illinois, Urbana, IL 61801, U.S.A.

Abstract—Measurements of entrainment and of droplet distributions are presented for air and water flowing in a horizontal 0.095 m pipe. A stratification of drops is observed because of the influence of gravity. Entrainment does not depend on pipe diameter and it increases strongly with increasing gas velocity. At small gas velocities, it is lower in horizontal pipes than in vertical pipes because gravitational settling enhances deposition.

1. INTRODUCTION

Gas–liquid flow in a pipeline at large gas velocities can result in a flow pattern for which a part of the liquid flows along the wall, W_{LF}, and a part as drops entrained in the gas, W_{LE}. Entrainment is defined as the ratio of the mass flow rate of entrained droplets to the total mass flow of liquid, $E = W_{LE}/W_L$. The prediction of E and of the distribution of liquid in the pipe plays an important role in understanding many practical problems.

This paper describes measurements of entrainment and of the distribution of droplet fluxes for air and water flowing in a horizontal 0.095 m pipeline at atmospheric pressure, and compares them with previous results for horiztonal and vertical pipes with different diameters. In vertical flows the liquid distributes symmetrically over the pipe cross-section. Because of gravitational effects in horizontal flows, the thickness of the liquid film and the droplet flux can have larger values at the bottom of the pipe. Consequently, a major concern of this paper is to show the effects of gravity and of pipe diameter on drop distribution and on entrainment.

Gas-phase turbulence and gas-phase stresses will increase with increasing inertia, $\rho_G U_{SG}^2$, where U_{SG} is the superficial gas velocity and ρ_G, the gas density. Gravitational effects will increase with $\rho_L gl$, where l is a characteristic length, such as the drop diameter or the average thickness of the liquid flowing along the wall. For simplicity, one can take l as equal to the pipe diameter, D. Therefore, asymmetries could be expected to increase with decreasing values of $(\rho_G/\rho_L)^{1/2}$ Fr, where Fr $= U_{SG}/(gD)^{1/2}$. Annular flow typically occurs for $U = 15$–200 m/s so large diameter pipes are characterized by lower $(\rho_G/\rho_L)^{1/2}$ Fr.

The effect of asymmmetries on entrainment will be discussed by comparing annular flows in vertical and horizontal pipes. Consequently, it is necessary to present a brief summary of correlations for a vertical system. Entrainment is considered as the result of a balance between the rate of atomization of the liquid film, R_A, and the rate of deposition of droplets, R_D. Under fully-developed conditions, $R_A = R_D$. Measurements of E in horizontal flows are interpreted by considering the effect of gravity on average values of R_A and R_D around the pipe circumference.

2. DESIGN RELATIONS FOR ENTRAINMENT

(a) Vertical flows

Taylor (1940) has shown that the rate of atomization associated with the flow of a gas over a thick water layer is given by

$$\tilde{R}_A = \frac{R_A}{U_G(\rho_G \rho_L)^{1/2}}$$ [1]

Equation [1] does not describe measurements for annular flows, for which $\tilde{R}_A$ is found to be a strong function of the mass flow of the liquid film, W_{LF}. If it is assumed that $\tilde{R}_A$ varies linearly with W_{LF}, then

$$\tilde{R}_A = k'_A (\Gamma) \qquad [2]$$

where $\Gamma = W_{LF}/\pi D$ and k'_A is an atomization constant. Results on deposition are, usually, correlated with the rate equation

$$R_D = k_D C_D \qquad [3]$$

where k_D is a deposition constant. The concentration of drops, in the units of mass per unit volume, is $C_D = W_{LE}/Q_G S$, with Q_G being the volumetric flow of the gas and S, the ratio of the drop and gas velocities. From [2] and [3] the following relation for entrainment under fully-developed conditions is obtained:

$$\frac{E}{1-E} = \frac{k'_A U_G^2 S D (\rho_G \rho_L)^{1/2}}{4 k_D} \qquad [4]$$

The above equation suggests that E is independent of liquid flow rate in regions where [2] and [3] are valid and where k_D is not dependent on the flow rate of the liquid film.

Measurements show that E is zero for $W_L < W_{LFC}$, where W_{LFC} is a critical flow rate of the liquid film below which atomization does not occur. Dallman *et al.* (1979) suggested that, at low Γ,

$$\tilde{R}_A = k_A U_G^n (\Gamma - \Gamma_0), \qquad [5]$$

where $k'_A = k_A U_G^n$ and $\Gamma_0 = W_{LFC}/\pi D$. Exponent n is unity for small D but it has a value of zero if $D \geqslant 2.54$ cm (Schadel *et al.* 1990). At large liquid flows, $\Gamma \gg \Gamma_0$; [2] is recovered. The influence of W_{LFC} on E can be taken into account by defining

$$E_M = 1 - \left(\frac{W_{LFC}}{W_L}\right). \qquad [6]$$

Equation [4] is, then, modified to give

$$\frac{(E/E_M)}{1-(E/E_M)} = \frac{k'_A U_G^2 S D (\rho_G \rho_L)^{1/2}}{4 k_D} \qquad [7]$$

The dependence of E on W_L at low W_L is taken into account through the dependency of E_M on W_L, given by [6]. Equations [3] and [5], with $n = 0$, have been verified, at low liquid flows ($\Gamma < 0.4$ kg/ms) by Schadel *et al.* (1990) for upward flow of air and water. They found that $k_A = 4.6 \times 10^{-4}$ ms/kg and that $Re_0 = 4\Gamma_0/\mu = 214, 299, 363$ for $D = 0.0254, 0.042, 0.0572$ m. An average value of $\Gamma_0 = 0.085$ kg/ms is obtained from these data.

Equation [7] shows no effect of liquid flow since it considered only results for small liquid flows. Andreussi (1983), Govan *et al.* (1988) and Schadel *et al.* (1990) show that k_D decreases with increasing droplet concentration at large flows. This causes E to increase. However, it is also expected that at large liquid flows k_A will decrease with increasing W_{LF}. This will cause E to decrease. The experiments of Schadel *et al.* show an increase of E with increasing liquid flow, so the decrease of k_D appears to be having a stronger effect than the decrease in k_A in this study.

(b) Characterization of asymmetries of the liquid film in horizontal flows

A number of investigators have studied the variation of the film height around the pipe circumference (Laurinat *et al.* 1985; Paras & Karableas 1991a; Fukano *et al.* 1983; Fukano & Ousaka 1989). A straightforward way to characterize the degree of asymmetry is to use the ratio of the film height at the top of the pipe to the film height at the bottom of the pipe, h_{180}/h_0. This has the disadvantage that h_{180}/h_0 mainly reflect variations in h_0.

Williams (1990) explored h_{45}/h_0 and $A_L/h_0 D$ as alternates. Here A_L is the cross-sectional area of the film, defined as

$$A_L = \int_0^\pi (D - 2h) h \, d\theta \qquad [8]$$

The latter choice was adapted in this paper because it uses all of the film height measurements and because it has interesting asymptotic behaviors. For a completely symmetric flow this parameter

has a value of $\pi(1 - 2m/D)$, where m is the spatially averaged height. An "ideal" stratified film is defined as one for which all of the liquid in the film flows along the bottom of the pipe with a horizontal interface. For small h this type flow gives a value of $(4/3)(h_0/D)^{1/2}$ for $A_L/h_0 D$, if the interface is perfectly horizontal. However, because of surface tension effects, h_0 will actually be smaller than what would be observed for a horizontal interface. Consequently, a lower asymptote of $A_L/h_0 D$ equal to $(4/3)(h_0/D)^{1/2}$ would be reached only for pipes with very large diameters. One would expect that $[A_L/h_0 D]/(4/3)(h_0/D)^{1/2}$ would increase with increasing $(\sigma/\rho g D^2)$, where δ is the surface tension.

(c) Rate of entrainment in horizontal flows

No information is available for the rate of atomization of the liquid layer for horizontal flows in a circular pipe. Consequently, it is attractive to assume that the local rate is given by [5], with $n = 1$, for low liquid flows. The average R_A is then obtained by integrating [5] around the pipe circumference. If the local film flow, Γ, is greater than Γ_0 at all locations

$$\langle R_A \rangle = k_A U_G (\rho_G \rho_L)^{1/2}\left(\frac{\langle W_{LF} \rangle}{\pi D} - \Gamma_0\right) \qquad [9]$$

where

$$\langle W_{LF} \rangle = \int_0^\pi D\Gamma \, d\theta \qquad [10]$$

The equation representing $\langle R_A \rangle$ is the same as [5] with $\langle W_{LF} \rangle$ replacing W_{LF}. If Γ does not exceed Γ_0 for $\theta > \theta_c$ then

$$\langle R_A \rangle = k_A U_G (\rho_G \rho_L)^{1/2}\left(\frac{\langle W_{LF} \rangle}{\pi D} - \Gamma_0^*\right) \qquad [11]$$

where

$$\Gamma_0^* = \Gamma_0 - \int_0^\pi (\Gamma_0 - \Gamma)D \, d\theta \qquad [12]$$

(d) Rate of deposition in horizontal flows

Binder & Hanratty (1991) have observed that concentration profiles for vertical annular flows are flat and concluded that deposition is controlled by free-flight to the wall, rather than turbulent diffusion. They assumed a Gaussian distribution for which the average magnitude of v is $(2/\pi)^{1/2}(\overline{v^2})^{1/2}$ and that one-half of the drops are moving toward the wall. Consequently, their results suggest that the local deposition constant is approximated by

$$k_D = (\overline{v^2})^{1/2}\sqrt{\frac{1}{2\pi}} \qquad [13]$$

where $\overline{v^2}$ is the mean-square of the fluctuations of the particle velocity in a direction perpendicular to the wall. Radial fluctuations of the fluid velocities can be approximated as $(\overline{u^2})^{1/2} \cong 0.9v^*$ where v^* is the friction velocity (Vames & Hanratty 1988). Therefore, [13] can be written as

$$k_D = C_1 v^* \frac{(\overline{v^2})^{1/2}}{(\overline{u^2})^{1/2}} \qquad [14]$$

where $C_1 \cong 0.9(2/\pi)^{1/2}$, $v^* = U_G(f/2)^{1/2}$ and f is the friction factor measured by Asali *et al.* (1985).

The rate of deposition in a horizontal annular flow will differ from a vertical annular flow because gravity, as well as turbulence, can contribute to deposition and because the droplet concentration field is not axisymmetric. From the results of Binder & Hanratty (1992), [13] for the local deposition constant should be modified as follows for a horizontal flow:

$$k_D = \frac{C_W}{C_B}[(\overline{v^2})^{1/2}(2\pi)^{-1/2} + V \cos\theta] \qquad [15]$$

where $\theta = 0$ is the bottom of the pipe, and C_B is the bulk concentration. The settling velocity, V, will reach a constant terminal velocity, V_T, if the particles have been in the field for a long enough time. The concentration at the wall, C_W, can vary with θ. The first term on the right side is the contribution due to turbulent velocity fluctuations and the second, due to gravitational settling.

At the top part of the pipe ($\theta > 90°$) gravity is opposing deposition and at the bottom of the pipe ($\theta < 90°$) gravity is aiding deposition. If $(C_W/C_B) = 1$ the net contribution due to gravitional settling would be zero. However, if C_W is larger at the bottom of the pipe, gravity would enhance the net deposition and could, even, be the dominant contributor.

An average value of k_D is given by

$$\langle k_D \rangle = F(\overline{v^2})^{1/2} \sqrt{\frac{1}{2\pi}} \qquad [16]$$

where

$$F = \frac{1}{\pi} \left\{ \int_0^\pi \frac{C_W}{C_B} \, d\theta + \int_0^\pi \sqrt{2\pi} \, \frac{V}{(\overline{v^2})^{1/2}} \frac{C_W}{C_B} \cos(\theta) \, d\theta \right\} \qquad [17]$$

is the ratio of $\langle k_D \rangle$ for a horizontal flow to k_D for a vertical flow, if $\overline{v^2}$ is the same.

3. DESCRIPTION OF EXPERIMENTS

The experiments in a 0.0953 m pipe were conducted in a flow loop described in a thesis by Williams (1990). The Plexiglas pipe was carefully aligned in the horizontal direction by measuring the liquid level in the pipe with no flow of air. The length was 26 m. Water and air were mixed at the inlet with a T section in which water flowed along the run. Measurements were made for a range of superficial air velocities of 26–88 m/s and superficial liquid velocities of 0.02–0.18 m/s. The pressure at the test section was 1.16 atm, so that $\rho_G = 1.4 \text{ kg/m}^3$.

Local film heights were measured using a conductance technique, described by Laurinat *et al.* (1985). The probes were made from two parallel 0.5 mm chrome wires separated by 5.1 mm and having a length of 15 mm. Plexiglas plugs inserted into the pipe wall were used to support the probes. The ends of the plugs were machined to be flush with the inside surface of the pipe. The accuracy of these measurements was about 5% and the minimum value of the film thickness that could be determined was 0.06 mm.

The local droplet flux was measured with a sampling tube with an internal diameter of 0.36 cm. A traversing mechanism positioned the tube at a desired location inside the pipe. The test section was specially designed so that it could be rotated to obtain flux-profiles at different angular orientations. The method used to measure drop fluxes is described in a paper by Asali *et al.* (1985) and in the thesis by Williams (1990). The sampling tube was also used to measure velocity profiles, as described by Dykhno *et al.* (1994).

Measurements of drop fluxes close to the liquid film are abnormally high because of sampling of the wave crests. Asali *et al.* (1985) ignored these data and used a linear extrapolation of the last two points to the average location of the wave interface. A power law extrapolation was used in this study because more points could be involved in a linear extrapolation on log–log co-ordinates. However, the differences in the results obtained with the two methods and with using no extrapolation was not greater than 15%.

Total entrainment fluxes, W_{LE}, can be obtained by integrating measurements of the local droplet flux over the cross-section. This approach is time-consuming, so a simpler method was explored. This involved the assumption that the liquid flux is not varying very much in the horizontal direction so that only the vertical profile needs to be used:

$$W_{LE} = C_2 \int_{h_0}^{D - h_{180}} F_{LE}(y) \frac{dA_G}{dy} \, dy \qquad [18]$$

where y is the distance from the bottom of the pipe, F_{LE} is the liquid flow per unit area measured by the sampling tube, h_0, h_{180} are the liquid heights at the bottom and top walls, and dA_G is the gas space area between y and $y + dy$. If $C_2 = 1$ the flux F_{LE} is independent of x. An effective value of C_2 can be obtained using the horizontal profile at $y = 0$, so that

$$C_2 = \frac{1}{F_{LE}^0(D - 2h_{90})} \int_{-(D/2 - h_{90})}^{(D/2 - h_{90})} F_{LE}(x, 0) \, dx \qquad [19]$$

Table 1. Calculations of entrainment with different procedures

U_{SG} (m/s)	U_{SL} (m/s)	W_{LE} (kg/s) 5 cross-sections	W_{LE} (kg/s) [18], $C_2 = 1$	W_{LE} (kg/s) [18], [19]
33	0.18	0.155	0.158	0.145

where $F_{LE}(x, 0)$ are the entrainment fluxes along $y = 0$, F_{LE}^0 is the entrainment flux at $x = 0$, $y = 0$. Another approach is to use a measurement at a single point.

A comparison of the total entrainment calculations with the different procedures is given in table 1. The value of W_{LE} in the third column was obtained by integrating droplet fluxes measured over the entire cross-section. The fourth column was obtained from [18] with $C_2 = 1$; the fifth column, from [18] and [19]. These results indicate that an accuracy within 5% can be realized by using only the vertical profile.

4. RESULTS

(a) Film height profiles

Figures 1 and 2 give plots of $A_L/h_0 D$ versus Fr and versus U_{SG}. These were obtained from measurements by Dallman (1978) in a 0.0254 m pipe and by Williams (1990) in a 0.0953 m pipe. The maximum gas velocity studied in both experiments was about 100 m/s. The values of Fr were twice as large for the smaller pipe as for the larger pipe at large U_{GS}. From the discussion in section 2(b) an upper limit for $A_L/h_0 D$ of about 3 is expected. (This would be smaller for small diameter pipes for which m/D could be significant.) From figure 3(a), it is seen that h_0/D has an upper
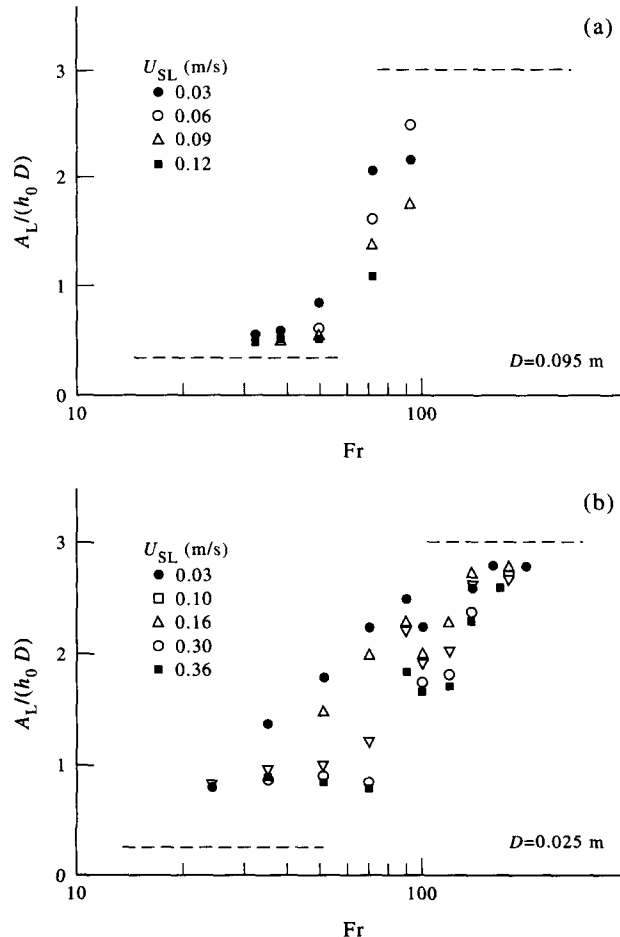
Figure 1. Effects of Froude number (Fr) and liquid flow rate on the film asymmetry parameter, $A_L/h_0 D$, for 0.095 m (upper) and 0.025 m (lower) horizontal pipes.
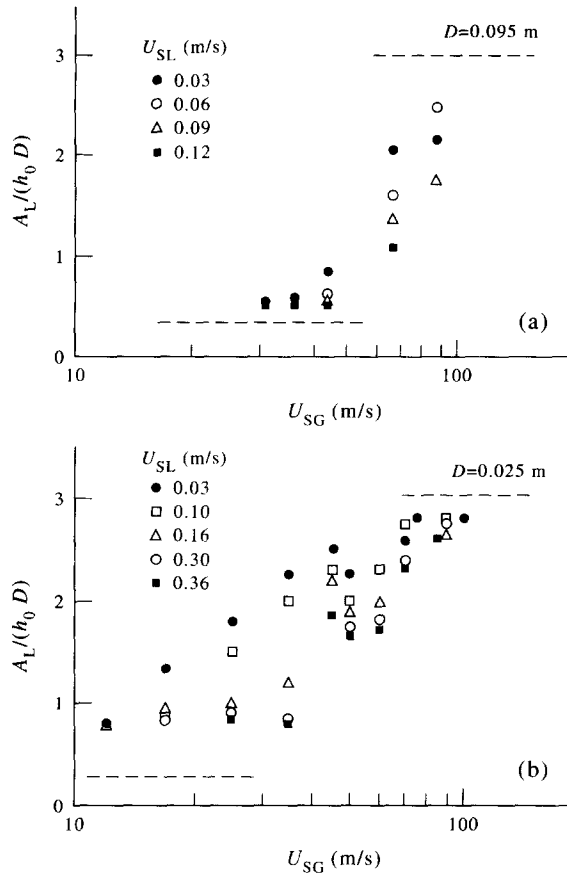
Figure 2. Liquid film asymmetry parameter, $A_L/h_0 D$, as a function of gas and liquid velocity for 0.095 m (upper) and 0.025 m (lower) horizontal pipes.

limit of about 0.06. Therefore $A_L/h_0 D$ would have a lower limit of about 0.33 for air and water flowing in a 0.0953 m pipe. In a similar way a lower limit of $(A_L/h_0 D) = 0.25$ is obtained for the 0.025 m pipe. These theoretical upper and lower limits are indicated in figures 1 and 2.

The values of $A_L/h_0 D$ are not accurate because of the limited number of measurements of h around the circumference. Nevertheless, they do show interesting trends. At $\mathrm{Fr} > 160$ the film height parameters have an upper asymptote of about 2.8 for the 0.025 m pipe, which is close to the theoretical value. Experiments in this region are classified as "symmetric" annular flows. The Froude numbers characterizing the flow in the 0.095 m pipe were not large enough for an upper asymptote to be established. Consequently, runs at high gas velocities are classified as "asymmetric annular flows" even though they given values of $A_L/h_0 D$ (2 to 2.5) close to the theoretical upper limit.

The measurements shown in figures 1 and 2 with $D = 0.095$ m have a lower limit of $A_L/h_0 D = 0.5$. Films giving this value are defined as stratified or stratified–annular, and would include half of the flows studied in the 0.095 m pipe. Only the experiments at $U_{SG} = 67$ and 88 m/s and the experiment with $U_{SL} = 0.03$ m/s, $U_{SG} = 45$ m/s do not fit this characterization.

Height profiles for $D = 0.095$ m and $U_{SG} = 31$ m/s are shown in figure 3(a). The profiles for $U_{SL} = 0.06$, 0.09, 0.12 m/s give $A_L/h_0 D = 0.5$. A cross section of the film for a typical stratified–annular flow is sketched in figure 4(a). It is noted that most of the liquid is flowing along the bottom wall. An idealized stratified flow with a horizontal interface is not observed. Figure 3(b) gives film profiles for $D = 0.095$ m for a fixed U_{SL} and different U_{SG}. The measurements for $U_{SG} = 31$, 37 m/s would be characterized as stratified ($A_L/h_0 D = 0.5$). The profile for $U_{SG} = 45$ m/s $(A_L/h_0 D = 0.6)$ is close to a stratified–annular condition and the profile for $U_{SG} = 88$ m/s $(A_L/h_0 D = 2.5)$ is close to a symmetric film. The cross section of the film for $U_{SG} = 88$ m/s and $U_{SL} = 0.06$ m/s, sketched in figure 4(b), is a typical asymmetric annular flow.
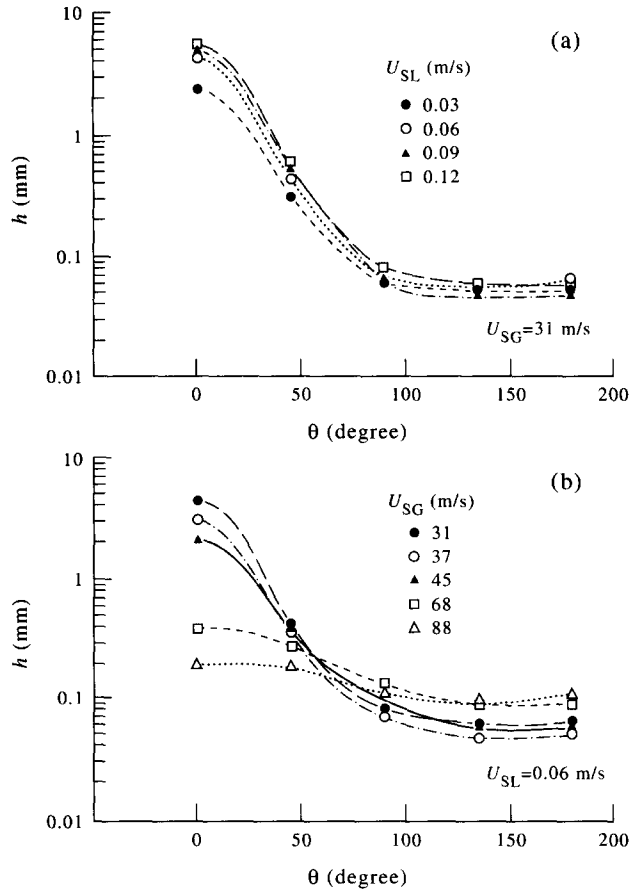
Figure 3. Liquid film thickness distributions at various liquid (upper) and gas (lower) velocities in a 0.095 m pipe.

The lower asymptote of $A_L/h_0 D = 0.75$, obtained for the experiments in the 0.025 m pipe (figures 1 and 2) is defined as characterizing a stratified or stratified–annular flow. Such flows are observed at $Fr < 90$ for large U_{SL}. These results (as well as those for $D = 0.095$ m) show that the asymmetry of the liquid film cannot be characterized only by $Fr = U_{SG}/(gD)^{1/2}$. Small liquid flows more easily form a symmetric film, while large liquid flows tend to stratify.

(b) Structure of profiles of droplet flux

Vertical profiles of local droplet flux, F_{LE}, are presented in figure 5(a) for a fixed superficial liquid velocity of $U_{SL} = 0.09$ m/s. At $U_{SG} = 26$ m/s, atomization is occurring but there is not a high enough deposition rate on the top wall to maintain a continuous film. This profile is characteristic of a non-wetting flow. There is a large decrease in droplet flux with increasing distance from the bottom wall. The droplet flux is low and relatively constant at the top of the pipe, indicating that gravity is having a weak effect on the drop distribution in this region. This could be explained if the diameters of drops are smaller in the top part of the pipe than in the bottom part for this flow.

An increase in the gas velocity from 26 to 31 m/s greatly increases droplet fluxes and creates large enough drop concentrations at the top of the pipe that the tube wall is completely wetted. According to measurements of $A_L/h_0 D$, shown in figures 1 and 2, the flux profiles for $U_{SG} = 31$, 37, 45 m/s in figure 5(a) would be associated with a liquid film which would be characterized as stratified–annular and the profiles for $U_{SG} = 67$, 88 m/s would be characteristic of an asymmetric annular flow.

However, the droplet profiles do not show as much asymmetry as do the film height profiles. For example, the fluxes at $U_{SG} = 37$, 45 m/s show variations of only about 2/1. The droplet fluxes for $U_{SG} = 67$, 88 m/s are varying only by a factor of about 1.5. Consequently, one would expect
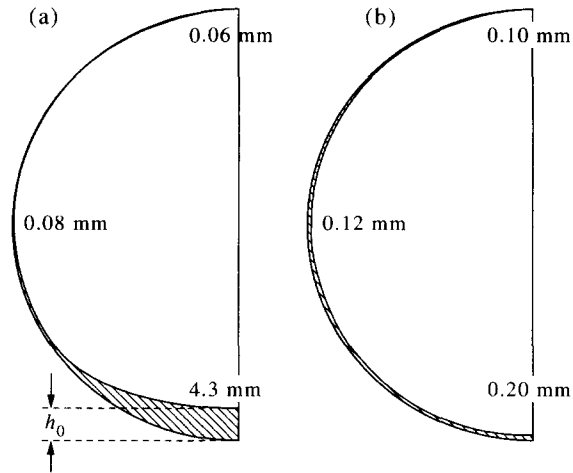
Figure 4. Sketches of liquid film thickness distribution around the pipe circumference at $U_{SG} = 31$, $U_{SL} = 0.06$ m/s (left) and $U_{SG} = 88$ m/s, $U_{SL} = 0.06$ m/s (right).
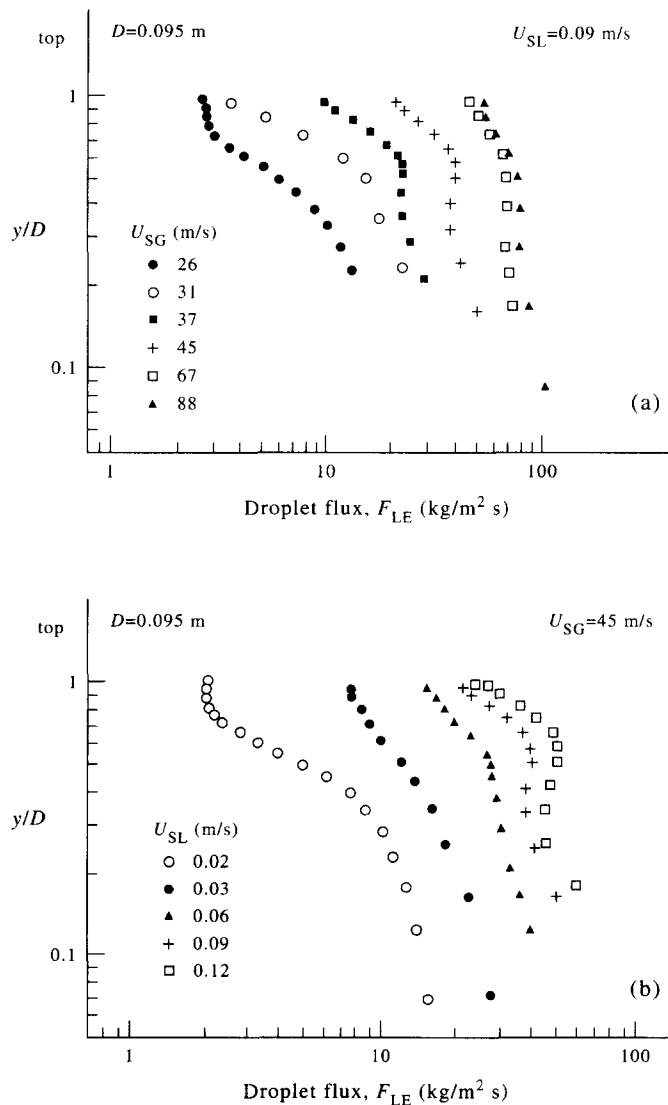
Figure 5. Vertical profiles of droplet flux at various gas (upper) and liquid (lower) velocities for a 0.095 m pipe.

| U_{SG}=26 m/s | U_{SG}=33 m/s | U_{SG}=45 m/s |
| U_{SL}=0.02 m/s | U_{SL}=0.18 m/s | U_{SL}=0.12 m/s |
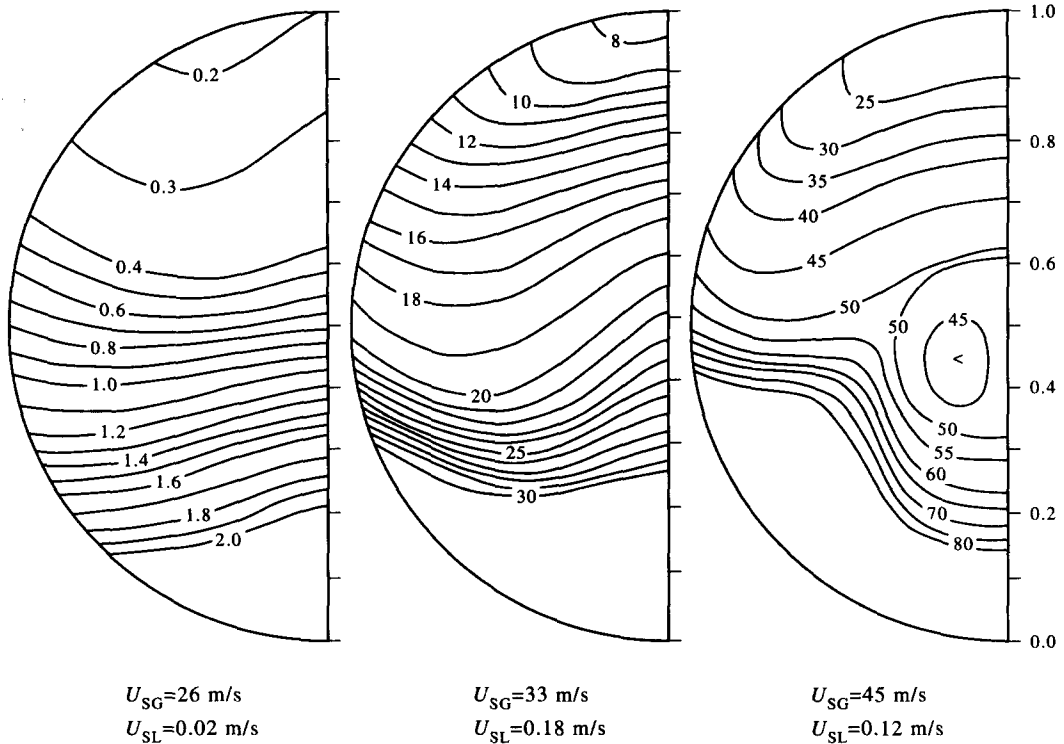
Figure 6. Contours of droplet flux at various gas and liquid velocities (kg/m^{2}s).

that average deposition rates for these two highest gas flows could be close to what is found in vertical annular flows.

An interesting aspect of the profiles shown in figure 5(a) is the appearance of a maximum at $y/d = 0.6$ for $U_{SG} = 37$ and 45 m/s. This type of behavior had previously been observed in horizontal flows (Dallman 1978; Williams 1986; Paras & Karabelas 1991b). Most likely it is a consequence of secondary flows in the gas which are tending to oppose droplet stratification. As shown by Dykhno et al. (1994), these flows are downward at the wall and upward at the center.

Figure 5(b) shows droplet fluxes for a fixed gas rate. At the lowest liquid flow, $U_{SL} = 0.02$ m/s, a non-wetting condition existed. A large increase in entrainment is observed with an increase of
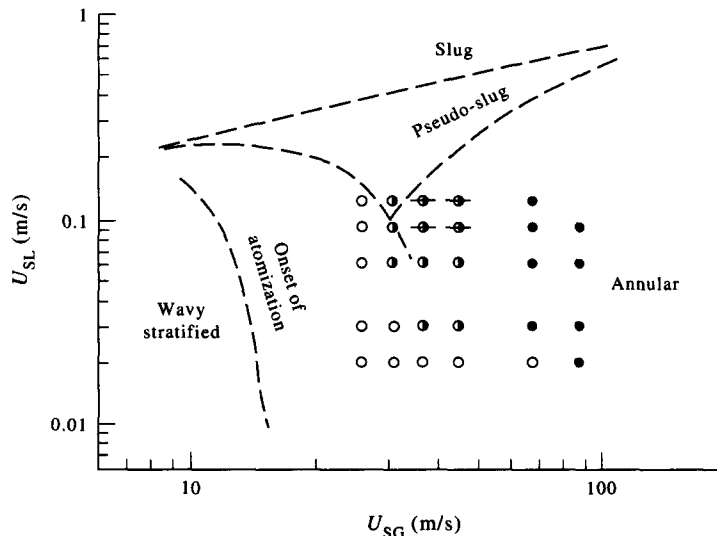
Figure 7. Flow regime map in terms of entrainment results: ○, stratified flow, non-wetted top wall; ◐, stratified–annular flow; ●, asymmetric annular flow; and ◑, droplet flux profiles with a "hump".

U_{SL} to 0.03 m/s and the tube wall is completely wetted. All of the profiles of film thickness are such that the flows could be characterized as stratified or stratified–annular. However, again droplet fluxes for $U_{SL} = 0.06, 0.09$ and 0.12 m/s are showing variations of only about 2 to 1. The appearance of a maximum at $y/D = 0.6$ is noted. This becomes more pronounced as the ratio of liquid to gas flow increases.

Mappings of droplet fluxes are shown in figure 6. The one for $U_{SG} = 26$ m/s, $U_{SL} = 0.02$ m/s represents a stratified flow for which the top wall is not wetted. A stratified–annular flow is depicted for $U_{SG} = 33$ m/s, $U_{SL} = 0.18$ m/s. The mapping for $U_{SG} = 45$ m/s, $U_{SG} = 0.12$ m/s represents a case for which a "hump" is observed in the vertical profile of droplet fluxes. According to figure 1 this flow would be characterized as a stratified-annular flow.

(c) Flow-regime map

Figure 7 summarizes the results on wall film thickness and droplet flux profiles discussed in the previous section. The dashed curves represent the flow regimes defined by Lin & Hanratty (1987) for air and water flowing in a 0.095 m pipe. Atomization is initiated at $U_{SG} = 10$–15 m/s. As the gas flow is increased more drops are generated and, eventually, the top wall becomes wetted and broad crested capillary ripples appear on the film. This transition is not reproducible since the wetting depends on the properties and previous history of the wall. Lin & Hanratty (1987), therefore, defined annular flow to occur when the film on the top wall was thick enough to sustain irregular three-dimensional waves (which they called a "turbulent" film). Clearly there should be a lower boundary on U_{SL}, at low U_{SG}, below which annular flow cannot exist. However, Lin & Hanratty did not explore this.
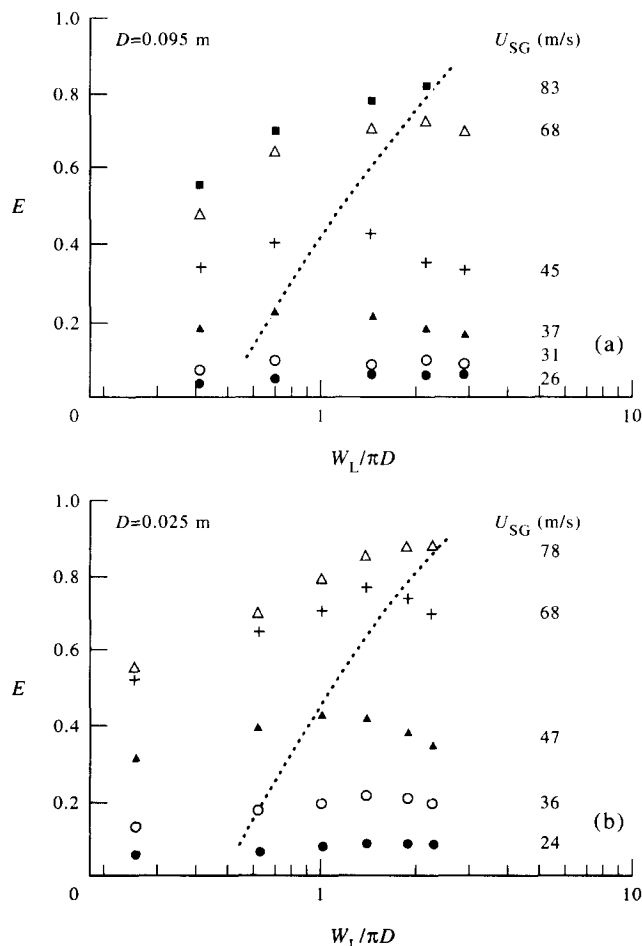
Figure 8. Effects of the liquid and gas flow rates on total entrainment in 0.095 m (upper) and 0.025 m (lower) pipes.

$D=0.095$ m $\qquad <E_0>\quad U_{SG}$ (m/s)

0.85   88
0.76   68
0.44   45
0.23   37
0.11   31 (a)
0.06   26

E/E_M

$W_L/\pi D$

$D=0.025$ m $\qquad <E_0>\quad U_{SG}$ (m/s)

0.85   78
0.75   68
0.42   47
0.20   36
0.08   24 (b)

E/E_M

$W_L/\pi D$
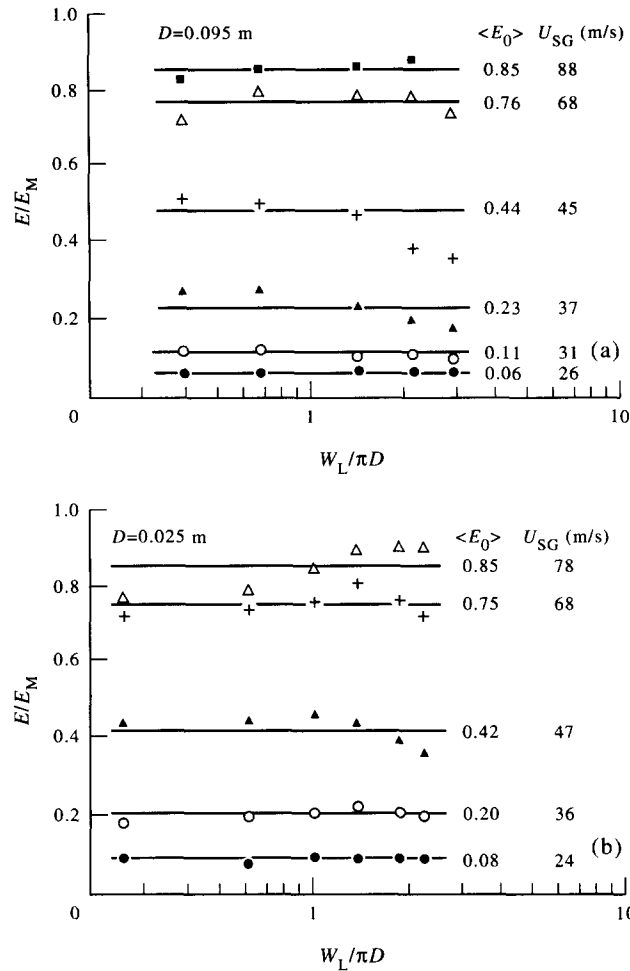
Figure 9. Total entrainment normalized with E_M for 0.095 m (upper) and 0.025 m (lower) pipes. Lines and numbers indicate the average values for a given gas velocity.

The points in figure 7 represent conditions for which droplet fluxes were measured. According to the film-distribution criterion in figure 1, all of the runs at $U_{SG} = 26\text{–}45$ m/s were stratified (or approximately stratified) except for the experiment at $U_{SG} = 45$ m/s, $U_{SL} = 0.12$ m/s. The open points represent droplet-flux profiles for non-wetting conditions, such as shown in figure 5(a) for $U_{SL} = 0.99$ m/s, $U_{SG} = 26$ m/s and in figure 5(b) for $U_{SG} = 45$ m/s, $U_{SL} = 0.02$ m/s. The darkened points represent asymmetric annular flows. The points that are partially darkened represent stratified flows for which the top wall was observed to be wetted. The points with arms are for conditions, with a large concentration of drops in the gas phase, for which "humps" appeared in the droplet flux profiles.

(d) Total entrainment

Measurements of the entrainment for the 0.095 m pipe are given in figure 8(a). Both annular flows and stratified flows with entrainment (wetting and non-wetting) are shown. The measurements are found to be, mainly, dependent on gas flow. At low liquid flows, the entrainment increases with increasing liquid flow, as has been found for vertical annular flows. This is particularly noticeable at conditions for which the droplets are more uniformly distributed over the pipe cross-section, $U_{SG} = 68$, 88 m/s.

An interesting aspect of these results is the decrease of E with increasing liquid flow observed at large liquid flows. For comparison, values of E for a 0.025 m pipe (Dallman 1978), are presented in figure 8(b). They were obtained from measurements of $\langle W_{LF} \rangle$, obtained by withdrawing the film through a porous section of wall. It is noted that pipe diameter appears to be having a small influence on E and that a drop-off occurs at large liquid flows.

The cause for this behavior is not known. The drop-off indicates that W_{LE} is not increasing as rapidly at W_L. One possibility is that drops increase in size with increasing liquid flow, either because of coalescence or because of an increase in the thickness of the wall layer. This could be associated with an increase in the settling velocity and, therefore, an increase in the deposition rate.

Another possibility is that at large enough values of $\langle W_{LF} \rangle / \pi D$ the equation for the rate of atomization departs from a linear dependency on W_{LF}, so that [9] overpredicts $\langle R_A \rangle$ (particularly, when the liquid layer in the bottom of the pipe is very thick). Support for this explanation is given in figure 8 where a dotted curve representing $W_{LF} / \pi D = 0.5$ kg/ms is plotted. This seems to correspond to the maximum E for the 0.025 m and the 0.095 m pipes for $U_{SG} > 35$ m/s.

As was the case for vertical configurations, the influence of liquid flow at small liquid flows can be removed if $E/E_M = E_0$ is plotted where

$$E_M = 1 - \frac{\langle W_{LFC} \rangle}{W_L} \qquad [20]$$

or

$$E_M = 1 - \frac{\pi D \Gamma_0}{W_L} \qquad [21]$$

Values of E_M with $\Gamma_0 = 0.13$ and 0.07 kg/ms have been used to analyze all of the results for the 0.095 and 0.025 m pipes, respectively. The results in figure 8 are replotted as E_0 in figure 9. As was found for vertical annular flows, the influence of liquid flow becomes less pronounced in this type of plot. The lines in figure 9 represent an average of measurements of E_0 for a fixed U_{SG}.

(e) Local entrainments, velocities and concentrations

The droplet flux profiles are presented in figure 10 as a local entrainment defined as

$$E_L = F_{LE} \bigg/ \frac{4 W_L}{\pi D^2},$$
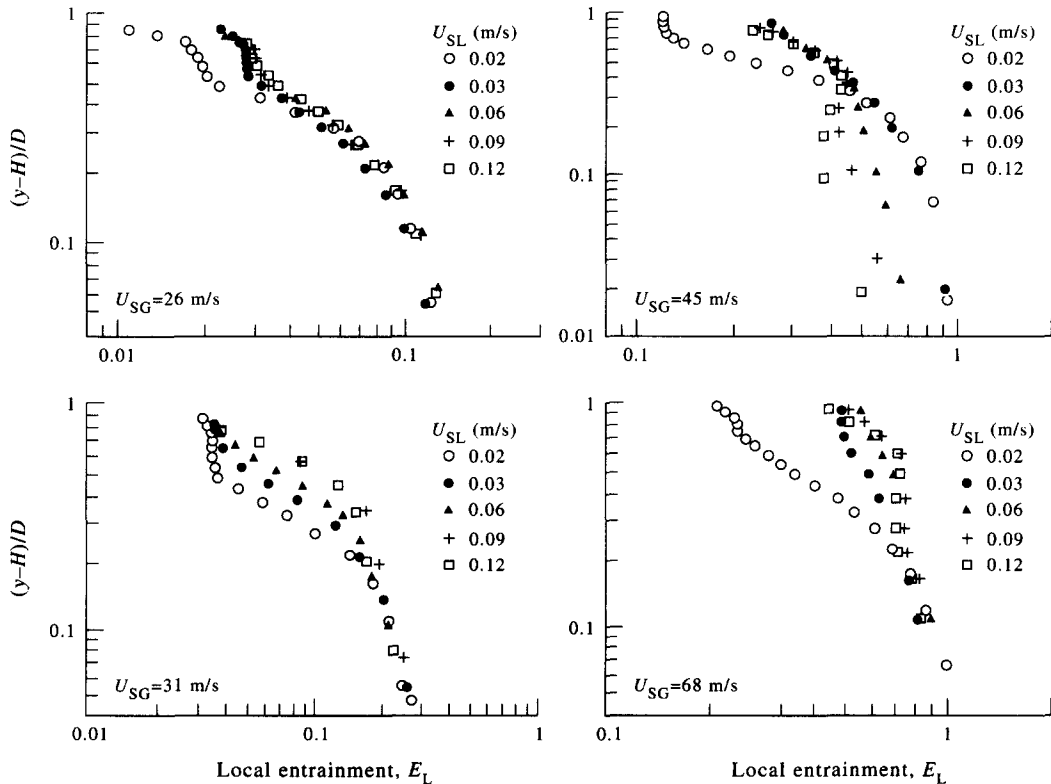
Figure 10. Local entrainment for different gas velocities: $U_{SG} = 26$ m/s (upper left), 31 m/s (lower left), 45 m/s (upper right) and 68 m/s (lower right).
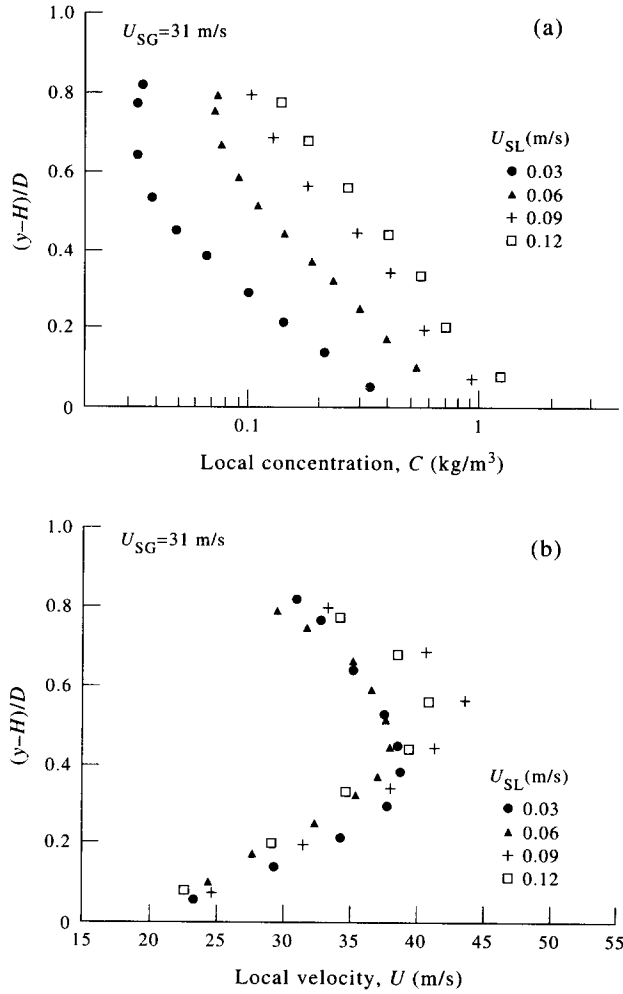
Figure 11. Vertical profiles of concentration (upper) and of velocity (lower) at $U_{SG} = 31$ m/s.

so that

$$E = \int_0^{A_G} E_L \, dA_G \qquad\qquad [22]$$

if C_2 in [18] is equal to unity. The dimensionless vertical co-ordinate is defined as $(y - H)/D$ instead of y/D. Term H is an average of the maximum values of the heights of disturbance waves.

The profiles for $U_{SG} = 26$ m/s are characteristic of flows for which the concentrations of drops are not sufficient to form a film at the top of the pipe. It is noted that, for $U_{SL} > 0.03$ m/s, F_{LE} increases linearly with W_L so that the entrainment profile does not change with increasing liquid flow. The profiles for $U_{SG} = 31$ m/s show a transition to conditions for which the tube wall is completely wetted ($U_{SL} > 0.06$ m/s). For $U_{SL} = 0.09$, 0.12 m/s the local entrainment seems to have reached a constant value. The data on E_L suggest that the drops in the gas flow are highly stratified; E_L has a range of values of about 8 to 1.

The results at $U_{SG} = 45$, 68 m/s show a different behavior, in that E_L is found to decrease at high enough U_{SG}. The profile for $U_{SL} = 0.03$ m/s, $U_{SG} = 45$ m/s has a similar shape to the one for $U_{SL} = 0.12$ m/s, $U_{SG} = 31$ m/s. Because of the larger E for the run at $U_{SG} = 45$ m/s, $U_{SL} = 0.03$ m/s the concentration of drops in the gas phase is roughly the same as for the run at $U_{SG} = 31$ m/s, $U_{SL} = 0.12$ m/s even though U_{SL} is only one-third as large. Increases in U_{SL} beyond 0.03 m/s are accompanied by large increases in the liquid film flow-rate and a drop in E_L. The drop in the total entrainment for these conditions is associated with a decrease in the local entrainment only in the lower half of the pipe. See, for example, profiles of E_L for $U_{SG} = 45$ m/s, $U_{SL} = 0.06$, 0.09, 0.12 m/s.

The measurements of E_L at $U_{SG} = 68$ m/s, however, show a decrease in E_L over the whole cross-section with an increase of U_{SL} from 0.09 to 0.12 m/s.

Some of the variation of droplet fluxes, shown in figure 5, can be associated with changes in local gas velocity. This is illustrated with measurements of profiles of droplet concentration and gas phase velocity in figures 11 and 12 for $U_{SG} = 31$ m/s and for $U_{SG} = 45$ m/s. The concentrations are defined as F_{LE}/SU_G. The local gas velocities, U_G, and an average ratio of droplet velocity to gas velocity, S, were determined by methods outlined by Williams (1990) and by Dykhno *et al.* (1994).

At $U_{SG} = 31$ m/s the concentrations increase with increasing liquid flow. They have a range of 10/1 from the bottom of the pipe to the top. At $U_{SL} = 0.03$, 0.06 m/s the velocity profile is roughly symmetric. At larger U_{SL} the highly roughened liquid layer at the bottom of the pipe is associated with a larger interfacial stress and a distortion of the velocity profile so that the maximum is displaced upward.

An increase of gas velocity to $U_{SG} = 45$ m/s causes a large increase in the concentration of drops. As pointed out by Dykhno *et al.* (1994) this increase in concentration is associated with a secondary pattern which has an upward flow in the center and a downward flow at the walls. This causes an upward displacement of the maximum in the velocity profile and an inflection in the concentration profile. Of interest is the observation that the concentration of drops close to the film on the bottom wall is roughly independent of liquid flow.
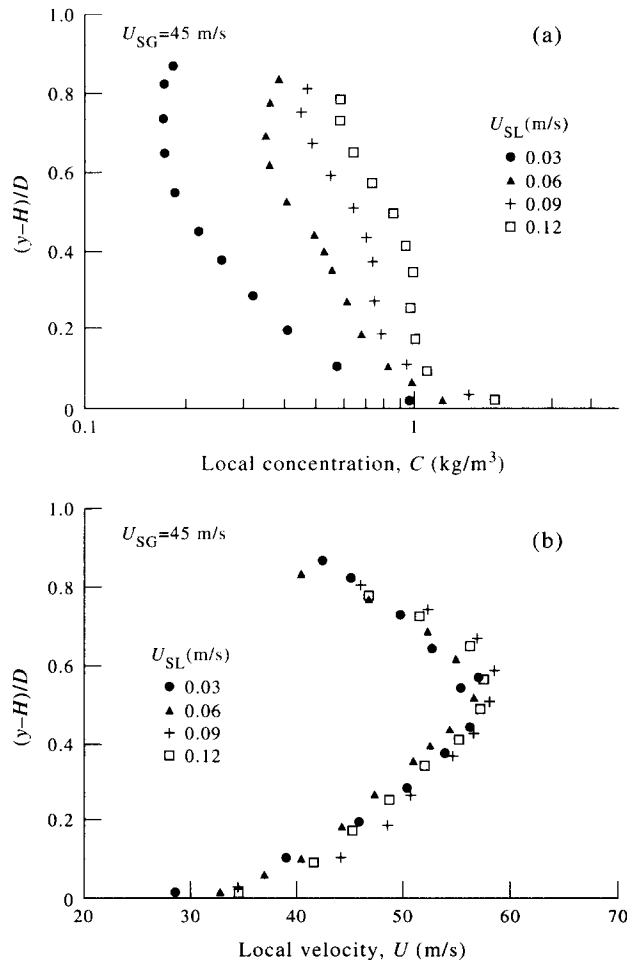
Figure 12. Vertical profiles of concentration (upper) and of velocity (lower) at $U_{SG} = 45$ m/s.
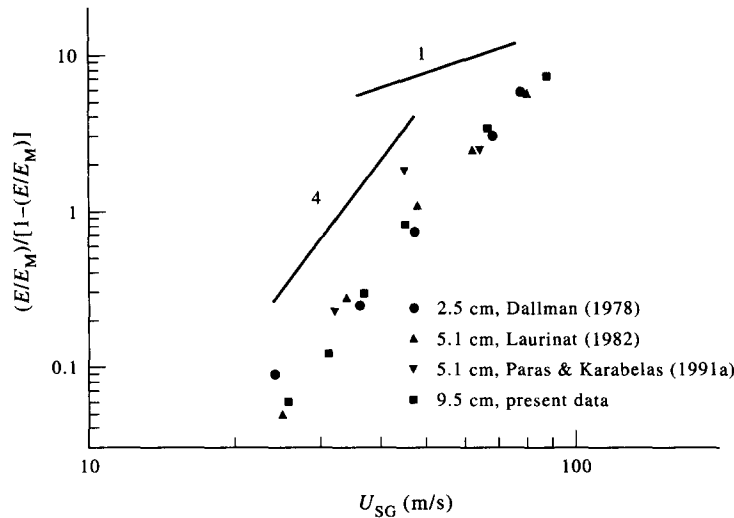
Figure 13. Effect of gas velocity on entrainment in horizontal pipes.

5. DISCUSSION

This paper presents measurements of entrainment and of droplet distributions for air–water annular flow in a 0.0953 m horizontal pipe. Gravity can cause a stratification of the droplets and a different behaviour of entrainment than is found in vertical pipes.

With increasing pipe diameter, at a constant gas velocity, the distribution of the liquid film around the pipe becomes more asymmetric. These measurements of film height suggest that a behavior similar to vertical annular flow should be realized when $(\rho_G/\rho_L)^{1/2}Fr$ is large enough. For air–water flow at atmospheric pressure, this occurs for $Fr > 160$. The focus of this paper is the behavior of annular flows for $Fr < 160$.

Droplets appear for $U_{SG} = 10$–20 m/s and for sufficiently large liquid flows that the film can be atomized. Flows with entrained drops can be subdivided into several regimes representing the distribution of liquid on the wall: a stratified flow for which there is insufficient drops at the top of the pipe to form a continuous liquid layer, a stratified–annular flow, an asymmetric annular flow and a symmetric annular flow.

Droplet flux profiles are consistent with measurements of the variation of the thickness of the liquid film; however they appear to be less asymmetric. This, in part, can be due to the additional mixing in the gas phase associated with a secondary flow that occurs when the conentration of
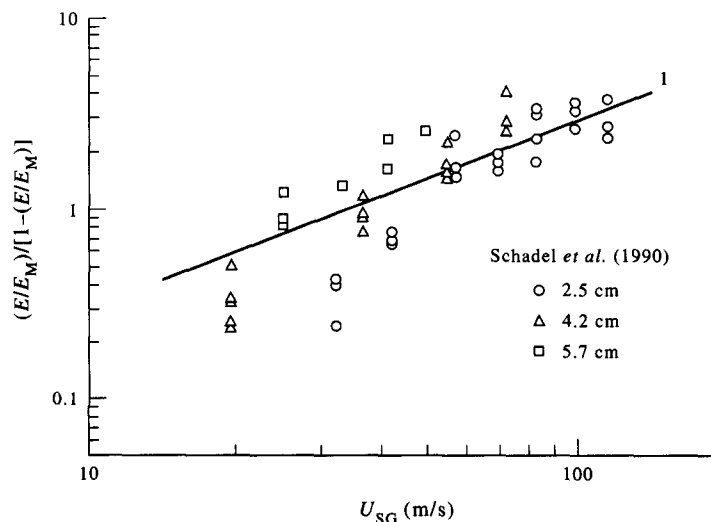
Figure 14. Effect of gas velocity on entrainment in vertical pipes.

drops is sufficiently high. Evidence of the influence of this secondary flow is the appearance of droplet flux profiles with a "hump", i.e. inflectional concentration profiles. The region of approximately constant concentration in the lower part of the pipe for high U_{SL} can be interpreted as occurring when the upward secondary flow counterbalances gravitational settling.

The prediction of the fraction of the liquid that appears in the gas phase, E, is of particular interest. These measurements are conveniently correlated as $E_0 = E/E_M$, where the maximum entrainment, E_M, takes into account that there is a minimum liquid flow in the wall layer below which atomization cannot occur. This normalized entrainment is affected mainly by gas velocity. An unanticipated result is an observed decrease in E or E_0 at large liquid flows. This could result from a number of causes. However, the observation that the drop in E occurs at the same value of $W_{LF}/\pi D$ for both the 0.025 m and the 0.095 m pipes suggests that it is associated with a departure of the rate of atomization from the linear relation ([9]). Of particular interest is the possbility that this drop in E with increasing liquid flow is the precursor of a transition to pseudo-slug or slug flow.

Average values of E_0, obtained as indicated in figure 9, are plotted as $E_0/(1 - E_0)$ in figure 13. The results for the 0.051 pipe are obtained from the thesis by Laurinat (1982) and the paper by Paras & Karabelas (1991a). The lines in figure 13 represent slopes of 1 and 4.

Equation [7] for vertical annular flows was developed for small liquid flows. It suggests that the influence of U_G and D on entrainment should be felt through the parameter $U_G^2 SD/U_G (f/2)^{0.5}$, since results from Schadel *et al.* suggest that $k_D \sim U_G (f/2)^{0.5}$ for small liquid flows. If S and $(f/2)^{0.5}$ are constants then $E_0/(1 - E_0)$ is predicted to vary as $U_G D$.

Measurements $E_0/(1 - E_0)$ by Schadel *et al.* for the upward flow of air and water in 2.5, 4.2 and 5.7 cm pipes are presented in figure 14 as a function of U_G. (Data for the very highest liquid flows where the entrainment showed an increase with increasing liquid flow are not used in this plot.) The line represents a slope of unity. The data for $U_{SG} > 40$ m/s are roughly in agreement with the prediction that $E_0/(1 - E_0) \sim U_G D$. The departure from that relation is interpreted by Schadel *et al.* as due to a decrease in S in small diameter pipes at low U_G.

A comparison of figures 13 and 14 shows that the results for horizontal flows differ from those for vertical flows in that they are not affected by pipe diameter and they show a much greater sensitivity to changes in gas flow. The independence of pipe diameter was unanticipated since the asymmetry of the wall layer at a given gas velocity is strongly affected by changes in pipe diameter.

The large increase of $E_0/(1 - E_0)$ with U_G can be understood by considering [16] and [17], describing deposition in horizontal flow. The equation for entrainment for small liquid rates can be written as

$$\frac{E_0}{1 - E_0} = N_H \tag{23}$$

where

$$N_H = \frac{k_A U_G^2 SD(\rho_G \rho_L)^{1/2}}{[(\overline{v_V^2})^{1/2}/(\overline{v_H^2})^{1/2}]} 4k_{DV} F \tag{24}$$

Term k_{DV} is the deposition constant for vertical flows and F is defined by [17]. For simplicity, the turbulence intensity will be assumed to be the same so that the chief difference between vertical and horizontal flows is the appearance of F.

The diameter D is in the numerator because, for fixed W_{LE} and W_{LF}, droplet concentration (or the rate of deposition) changes as D^{-2} and Γ (or the rate of atomization) changes, as D^{-1}. The independence of E_0 of pipe diameter could, therefore, be explained because increases in F with D offsets the influence of pipe diameter outlined above.

A consideration of F in the limit of large V gives

$$k_D = \frac{1}{\pi} V \int_0^\pi \frac{C_W}{C_B} \cos(\theta) \, d\theta \tag{25}$$

If the drag force on the drops is described by Stokes law and V can be approximated by V_T, then

$$V = \frac{g d_p^2 \rho_L}{\mu_G} \tag{26}$$

Tatterson *et al.* (1977) give the following estimate for the effect of system variables on drop size:

$$d_p = D^{1/2}\left(\frac{\sigma}{\rho_G U_G^2 f_S}\right)^{1/2} \qquad [27]$$

where f_S is the friction factor for flow over a smooth wall and σ is the surface tension. The substitution of [26] and [27] into [25] gives

$$k_D \sim \frac{g\rho_L D}{\mu_G}\left(\frac{\sigma}{\rho_G U_G^2 f_S}\right)\left\langle\frac{C_W}{C_B}\right\rangle \qquad [28]$$

where

$$\left\langle\frac{C_W}{C_B}\right\rangle = \frac{1}{\pi}\int_0^\pi \frac{C_W}{C_B}\cos(\theta)\,d\theta \qquad [29]$$

The substitution of [28] into [7] gives

$$\frac{E_0}{1-E_0} \sim U_G^4\left(\frac{\mu_G\rho_G}{g\sigma}\right)\sqrt{\frac{\rho_G}{\rho_L}}\frac{k_A S f_S}{\langle C_W/C_B\rangle} \qquad [30]$$

If the effects of gas velocity and pipe diameter on S, f_S and $\langle C_W/C_B\rangle$ are ignored, [30] indicates $E_0/(1-E_0)$ varies with U_G^4 and is independent of D at small U_{SG}, in agreement with figure 13. Of course, the result in [30] is an approximation because of the simplifications used and because [27] has not been properly tested. Consequently, the method for estimating the effect of D is open to question. Nevertheless, one can conclude from this derivation that the strong effect of gas velocity on entrainment in horizontal gas–liquid flows is the result of the influence of gravitational settling on the deposition of drops. This settling velocity decreases with increasing U_G because of a decrease in drop size.

REFERENCES

Andreussi, P. 1983 Droplet transfer in two-phase annular flow. *Int. J. Multiphase Flow* **9**, 697–713.

Asali, J. C., Leman, G. W. & Hanratty, T. J. 1985 Entrainment measurements and their use in design equations. *PCH Phys. Chem. Hydrodynam.* **6**, 207–221.

Binder, J. L. & Hanratty, T. J. 1991 A diffusion model for droplet deposition in gas/liquid annular flow. *Int. J. Multiphase Flow* **17**, 1–11.

Binder, J. L. & Hanratty, T. J. 1992 Use of Lagrangian methods to describe drop deposition and distribution in horizontal gas–liquid annular flows. *Int. J. Multiphase Flow* **18**, 803–820.

Dallman, J. C. 1978 Investigation of separated flow model in annular gas–liquid two-phase flows. Ph.D. thesis, University of Illinois, Urbana, IL.

Dallman, J. C., Jones B. G. & Hanratty, T. J. 1979 Interpretation of entrainment measurements in annular gas–liquid flow. In *Two-phase Momentum Heat and Mass Transfer* (Edited by Durst, F., Tsiklauri, G. V. & Afgan, N. H.), Vol. 2, pp. 681–693. Hemisphere, Washington, DC.

Dykhno, L. A, Williams, L. R. & Hanratty, T. J. 1994 Maps of mean gas velocity for stratified flow with and without atomization *Int. J. Multiphase Flow* **20**, 691–702.

Fukano T. & Ousaka, A. 1989 Prediction of circumferential distribution of film thickness in horiontal and near-horizontal gas–liquid annular flow. *Int. J. Multiphase Flow* **15**, 403–420.

Fukano, T., Ousaka, A., Morimoti, T. & Sekoguchi K. 1983 Air–water annular two-phase flow in a horizontal tube. *Bull. JSME* **26**, 1387–1395.

Govan, A. H., Hewitt, G. F., Owen, D. G. & Bott, T. R. 1988 An improved CHF modelling code. *2nd U.K. National Heat Transfer Conf.*, Strathclyde University, Glasgow, pp. 33–48.

Laurinat, J. E. 1982 Studies of the effects of pipe size on horizontal annular two-phase flows. Ph.D. thesis, University of Illinois, Urbana, IL.

Laurinat, J. E., Hanratty, T. J. & Jepson, W. P. 1985 Film thickness distribution for gas–liquid annular flow in a horizontal pipe. *PCH Phys. Chem. Hydrodynam.* **6**, 179–195.

Lin, P. Y. & Hanratty, T. J. 1987 Effect of pipe diameter on flow patterns for air–water flow in horizontal pipes. *Int. J. Multiphase Flow* **13,** 549–563.

Paras, S. V. & Karabelas, A. J. 1991(a) Properties of the liquid layer in horizontal annular flow. *Int. J. Multiphase Flow* **17,** 439–454.

Paras, S. V. & Karabelas, A. J. 1991(b) Droplet entrainment and deposition in horizontal annular flow. *Int. J. Multiphase Flow* **17,** 455–468.

Schadel, S. A., Leman, G. W., Binder, J. E. & Hanratty, T. J. 1990 Rates of atomization and deposition in vertical annular flow. *Int. J. Multiphase Flow* **16,** 363–374.

Tatterson, D. F., Dallman, J. C. & Hanratty T. J. 1977 Drop sizes in annular gas–liquid flows. *AIChE J.* **23,** 68–76.

Taylor, G. I. 1940 Generation of ripples by wind blowing over a viscous fluid. "The Scientific Paper of Sir Geoffrey Ingram Taylor", Cambridge University Press, pp. 244–254.

Vames, J. S. & Hanratty T. J. 1988 Turbulent dispersion of droplets for air flow in a pipe. *Exp. Fluids* **6,** 94–104.

Williams, L. R. 1986 Entrainment measurements in a 4-inch horizontal pipe. M.Sc. thesis, University of Illinois, Urbana, IL.

Williams, L. R. 1990 Effect of pipe diameter on horizontal annular two-phase flow. Ph.D. thesis, University of Illinois, Urbana, IL.